Conceptual Design of HFIR Irradiation Experiment for Material Compatibility Study on Liquid Sn Divertor*)

Masatoshi KONDO, Bruce A. PINT[1)], Jiheon JUN[1)], Nick RUSSELL[1)], Joel McDUFFEE[1)], Masafumi AKIYOSHI[2)], Teruya TANAKA[3)], Naoko OONO[4)], Junichi MIYAZAWA[3)], Josina W GERINGER[1)], Yutai KATOH[1)] and Yuji HATANO[5)]

Tokyo Institute of Technology, Ookayama, Meguro-ku, Tokyo 152-8550, Japan
[1)]*Oak Ridge National Laboratory, Oak Ridge, TN 37831, United States of America*
[2)]*Osaka Prefecture University, 1-1 Gakuen-cho, Naka-ku, Sakai, Osaka 599-8531, Japan*
[3)]*National Institute for Fusion Science, 322-6 Oroshi-cho, Toki, Gifu 509-5292, Japan*
[4)]*Hokkaido University, Kita 8, Nishi 5, Kita-ku, Sapporo, Hokkaido 060-0808 Japan*
[5)]*University of Toyama, 3190 Gofuku, Toyama 930-8555, Japan*

(Received 2 November 2020 / Accepted 8 February 2021)

Liquid Sn is one of the promising coolants for liquid surface divertor concept of fusion reactors. However, the compatibility between liquid Sn and structural materials is an important issue that has to be addressed, because liquid Sn is extremely corrosive to steels at high temperatures. The corrosion may be mitigated when a protective Al_2O_3 layer is formed on the surface of alumina forming steels. However, the effect of neutron irradiation on the integrity of protective layer is not made clear so far. Japan and US joint research project "FRONTIER" started in 2019 to investigate the material compatibility under neutron irradiation. The purpose of the present study is to develop the conceptual design of the irradiation test capsule which enables material compatibility tests for the alumina forming steels – liquid metal systems under neutron irradiation in the High Flux Isotope Reactor at Oak Ridge National Laboratory, TN, USA. The three dimensional drawing of capsule structure was then developed. The validity of the material selections for the capsule design was investigated by means of corrosion tests of SiC, Si_3N_4, Ti, and Mo in liquid Sn at 773 K for 262 hr.

Keywords: liquid metal, irradiation, divertor, compatibility, irradiation test capsule

DOI: 10.1585/pfr.16.2405040

1. Introduction

Liquid metal tin (Sn) is one of the promising coolants for the liquid surface divertor of fusion reactors [1, 2] due to its excellent thermophysical properties and low vapor pressure [3]. However, the chemical compatibility between liquid Sn and structural materials is an important issue that has to be addressed. Liquid Sn is extremely corrosive to steels at high temperatures. Steels corrodes in liquid Sn due to the dissolution type corrosion and the formation of intermetallic compounds [4, 5].

The corrosion resistance of FeCrAl alloys has been investigated. They form alumina (Al_2O_3) layer on their surface, which is thermodynamically stable and chemically compatible with liquid metals Pb-Bi [6] and Pb-16Li [7]. The Al_2O_3 layer worked as a diffusion barrier against liquid Sn [8].

The effect of neutron irradiation on the integrity of the protective Al_2O_3 layer has not been investigated so far. The neutron irradiation induces the formation of point defects, such as interstitials and vacancies, interstitial and vacancy type dislocation loops, and voids inside the layer structure [9]. These neutron damages may degrade the barrier function of the Al_2O_3 layer. The corrosion acceleration kinetics has not been made clear, though it is important concern not only for the liquid surface divertor concept but also for the liquid breeder blanket system. Japan and US joint research project "FRONTIER" started in 2019 to investigate the reaction dynamics at interfaces in DEMO divertor systems and irradiation effects, and the TASK 3 focused on the chemical compatibility of Al-bearing ODS alloys and some other corrosion resistant materials with liquid metals under neutron irradiation [10].

The purpose of the present study is to develop the conceptual design of the irradiation test capsule which enables material compatibility tests for the alumina forming steels – liquid metal Sn systems under neutron irradiation in the High Flux Isotope Reactor (HFIR) at Oak Ridge National Laboratory, TN, USA. A rabbit capsule for liquid Sn experiment at HFIR was deigned, and its key features such as corrosion test methodologies under neutron irradiation and chemical compatibility of capsule materials were investigated.

author's e-mail: kondo.m.ai@m.titech.ac.jp
*) This article is based on the presentation at the 29th International Toki Conference on Plasma and Fusion Research (ITC29).

2. Conceptual Design of Irradiation Capsule in HFIR

The design of liquid Sn rabbit capsule which enables to perform compatibility tests under neutron irradiation in HFIR was developed. Figure 1 shows the three dimensional drawing of capsule structure by CREO Parametric. Three SS-3 samples of FeCrAlZr-ODS alloys after pre-oxidation treatment and silicon carbide (SiC) thermometry [11] are installed in the internal holder of the rabbit capsule.

Figure 2 shows the procedures of the corrosion test in liquid Sn under neutron irradiation in HFIR. Solid Sn of approximately 2 cc is installed in the internal holder in an inert atmosphere as shown in Fig. 2 (a). The solid Sn is melted onto the corrosion specimens by nuclear heating during the neutron irradiation as shown in Fig. 2 (b). Figure 3 shows the dose rates by Gamma and X rays of liquid materials (1 g) after 1 cycle (24 days) irradiation in HFIR, which were calculated with FISPACT-2005 [12]. Here, the irradiation experiment of the capsule is assumed to be performed in the unshielded removable beryllium (RB) position of HFIR. The fast neutron fluence is assumed to be 1×10^{25} n/m^2 (E > 0.1 MeV) [13]. The does rate of ODS FeCrAlZr alloy which has chemical composition of Fe-14.76Cr-6.4Al-0.5Ti-0.37Y-0.32O-0.37Zr was shown in Fig. 3. Co impurity contained in the normal steels is typically 500 mass ppm and controls several-years dose rate in the typical post-irradiation tests. The dose rates of the alloy with Co impurity of 0, 100, and 500 mass ppm were also calculated. The effect of the Co impurity on the dose rate was shown in Fig. 3. The dose rate of Sn is larger than the other liquid materials. Therefore, the dose rate of the specimens will be higher if solidified Sn remains on the specimens. Therefore, the solidified Sn must be removed from the specimen for further metallurgical analysis in the Low Activation Materials Development and Analysis (LAMDA) facility at ORNL. Therefore, the capsule is inverted and heated to remove the melted Sn from the specimens in the hot cell as shown in Fig. 2 (c). The capsule is then disassembled and the specimens are taken out from the internal holder for post irradiation characterization at LAMDA (Fig. 2 (d)). The mass loss of the specimens is measured and the corrosion attack on the specimens is metallurgically analyzed.

The temperature of liquid Sn is kept at 673 K for a period of 22 to 26 days as one operating cycle of the neutron irradiation experiment in HFIR. The accidental leakage of liquid Sn from the internal holder due to the corrosion during the reactor operation must be prevented. The internal holder must be made of corrosion resistant material against liquid Sn. The chemical compatibility of candidate materials for the internal holder was investigated by means of corrosion tests in liquid Sn at a static condition. Unalloyed Ti has commonly been used for the internal capsule fabrication. The corrosion resistance of Si_3N_4 [14] and refractory metals such as Mo and W [15, 16] in liquid metals has been reported, and they may also be suitable for the material of the internal holder. However, the information is still limited.

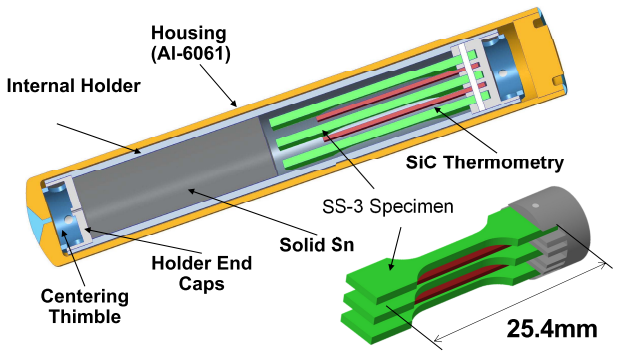

Fig. 1 Liquid Sn rabbit capsule for compatibility study under neutron irradiation in HFIR.

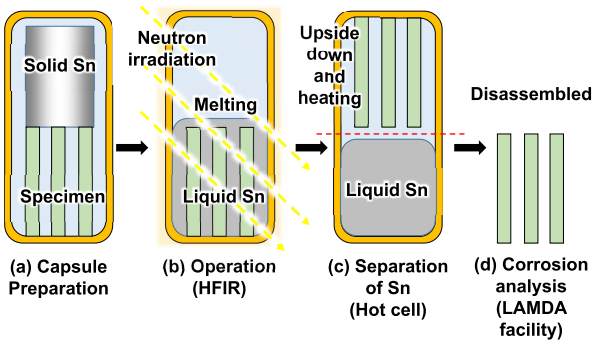

Fig. 2 Preparation and disassemble of liquid Sn rabbit capsule.

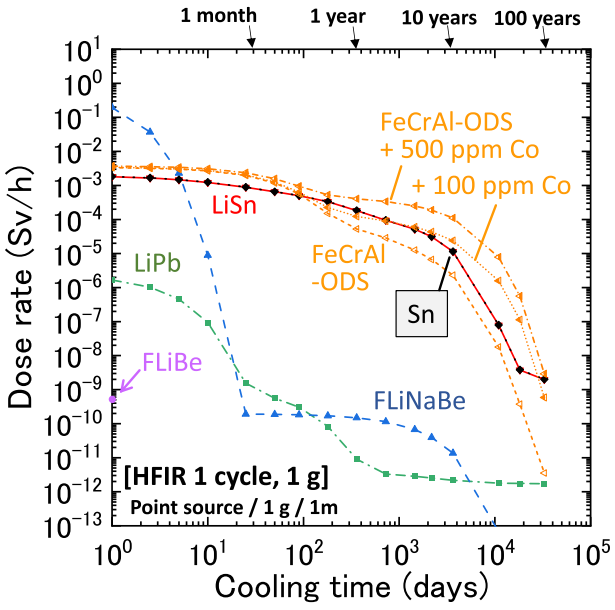

Fig. 3 Dose rates by Gamma and X rays of materials after 1 cycle (24 days) irradiation in unshielded removable beryllium (RB) position of HFIR (Fast neutron fluence is assumed to be 1×10^{25} n/m^2 (E > 0.1 MeV) [13]).

The capsule housing made of A6061 (Al-Mg-Si) must stand even in the situation where liquid Sn accidentally leaks from the internal holder and contacts with the housing. The temperature of the housing is kept at 323 K by cooling its outside during the irradiation test in the current capsule design. Liquid Sn which contacts with the capsule housing can be cooled and solidified within a short time. However, the Al-Sn phase diagram indicates that liquid Sn can chemically react with Al due to the solid solution of Al into Sn. The chemical reaction between liquid Sn and Al at 323 K was investigated by means of liquid Sn dripping experiment.

3. Chemical Compatibility of Liquid Sn with Capsule Materials

3.1 Experimental conditions

The corrosion of SiC, Si_3N_4, Ti, W, and Mo in liquid Sn was investigated by means of static corrosion tests. The test conditions were summarized in Table 1. The rectangular specimen was installed with liquid Sn in the crucible made of 316L austenitic steel (Fe-18Cr-12Ni-2Mo) as shown in Fig. 4 (a). The test setups were installed in the vessel filled with Ar having a purity of 99.99% and kept at 773 K by heater wound around the vessel. The detailed structure of test apparatus was reported in the previous articles [4, 8]. The corrosion resistance of W in liquid Sn at 773K was reported in our previous article [16].

The test setup was heated to the melting point of Sn after the test, and liquid Sn and the specimen was then taken out from the crucible. The specimen surfaces and their cross sections were metallurgically analyzed by field emission type scanning electron microscope and energy dispersive X-ray spectrometry (FE-SEM/EDX). The Si_3N_4 specimen was analyzed by auger electron spectroscopy (AES). Only the Mo specimen was cleaned with liquid Li and adhered Sn was removed from its surface. The mass loss due to the corrosion was then measured using an electro reading balance with an accuracy of 0.1 mg.

The chemical interaction between liquid Sn and Al for a short time was simulated by means of dripping experiment as shown in Fig. 4 (b). The plate made of pure Al was installed on the plate heater, and the temperature was kept at 323 K. Liquid Sn of 2 cc at 673 K was dripped onto the plate. The temperature change of the plate surface was measured by the thermocouple. The behavior of liquid Sn and the damage of the Al plate was observed.

3.2 Corrosion resistance of SiC and Si_3N_4 in liquid Sn

Figures 5 shows the results of visual inspection of the specimens after the tests. The SiC and Si_3N_4 specimens did not change its color by the exposure to liquid Sn. Adhered Sn was easily removed from the specimen surface. The wettability of liquid Sn on SiC was poor, and this feature was almost the same with that of Al_2O_3 bulk [8]. The

Table 1 Experimental conditions of corrosion tests with SiC, Si_3N_4, Ti, W [16], and Mo in liquid Sn.

	Temperature [K]	Time [hours]	Specimen size [mm]
SiC	773	262	10 × 15 × 2.3
Si_3N_4		262	10 × 15 × 2
W [17]		250	10 × 15 × 2.45
Ti		262	10 × 15 × 2
Mo		250	10 × 15 × 0.9

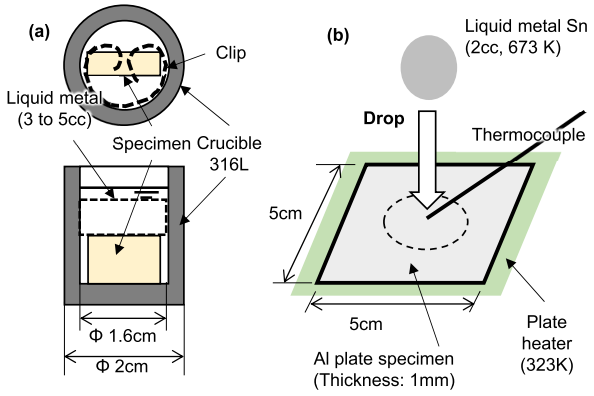

Fig. 4 (a) Test setup for static corrosion test, and (b) liquid metal contact test.

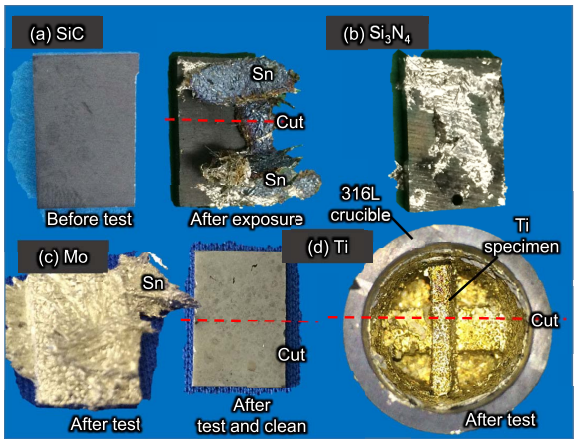

Fig. 5 SiC, Ti, and Mo specimens after exposure to liquid Sn at at 773 K for 262 hr.

poor wetting indicated a small force of chemical and thermodynamic interaction between liquid Sn and these materials.

Figures 6 shows the result of cross sectional SEM/EDX analysis on the surface of SiC specimen after the test. The depletion of Si and the enrichment of oxygen on the specimen surface were detected. The surface was slightly oxidized due to the chemical reaction with oxygen dissolved in liquid Sn. The oxidation was possibly caused by the inward diffusion of oxygen into SiC. Carbon was then left and enriched below the oxidation layer. The carbon peak obtained in the EDX result located slightly

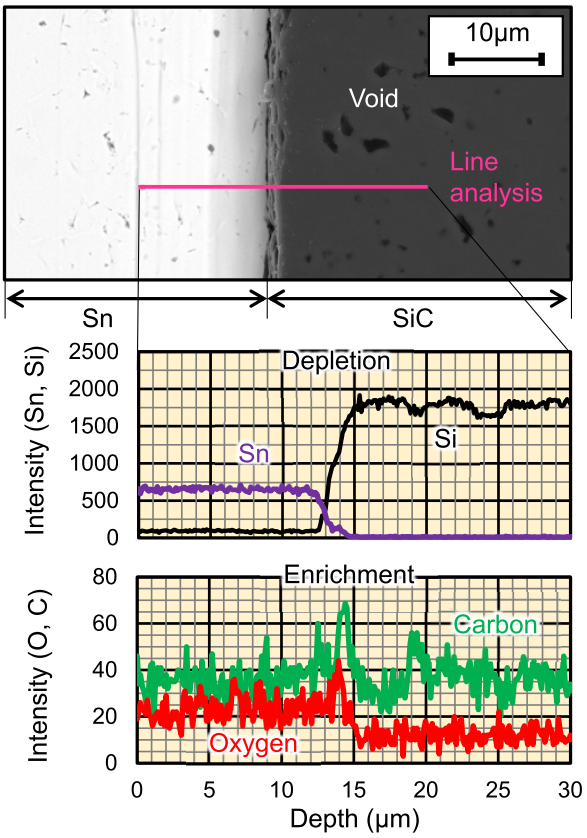

Fig. 6 Cross sectional SEM/EDX analysis of SiC specimen after exposure to liquid Sn at 773 K for 262 hr.

inward from the oxidation layer. The possible oxidation reaction [1] is;

$$SiC + 2O_{(Sn)} \rightarrow SiO_2 + C. \quad (1)$$

Liquid Sn forms SnO_2 as primary oxide when the oxygen saturates in liquid Sn. The chemical potential of oxygen ($\Phi_{O,Sn}$ [kJ/atom O]) in liquid Sn can be expressed as

$$\Phi_{O,Sn} = \frac{1}{2}\Delta G^{o}_{f,SnO_2} + RT\ln\left(\frac{C}{Cs}\right), \quad (2)$$

where C is the oxygen concentration [wt%], Cs is the oxygen solubility [wt%], $\Delta G^{o}_{f,SnO2}$ is the standard Gibbs free energy of formation of SnO_2 [kJ/mol], R is the gas constant (8.314×10^{-3} [kJ/K/mol]), and T is the liquid temperature [K]. Figure 7 shows the relationship between chemical potential of oxygen in liquid Sn and standard Gibbs free energy for formation of some oxides [17]. The chemical potential of oxygen in liquid Sn corresponds to the standard Gibbs free energy for formation of SnO_2 per one oxygen atom, when the oxygen saturates in liquid Sn ($C/Cs = 1$). It becomes lower at lower oxygen concentration. Though the oxygen concentration in liquid Sn was not measured in the present study, the chemical potential at possible oxygen concentration ($C/Cs = 0.01$) was estimated and indicated by dashed line in Fig. 7 as an example. The oxygen potential is seemed to be much higher than that of SiO_2 even at

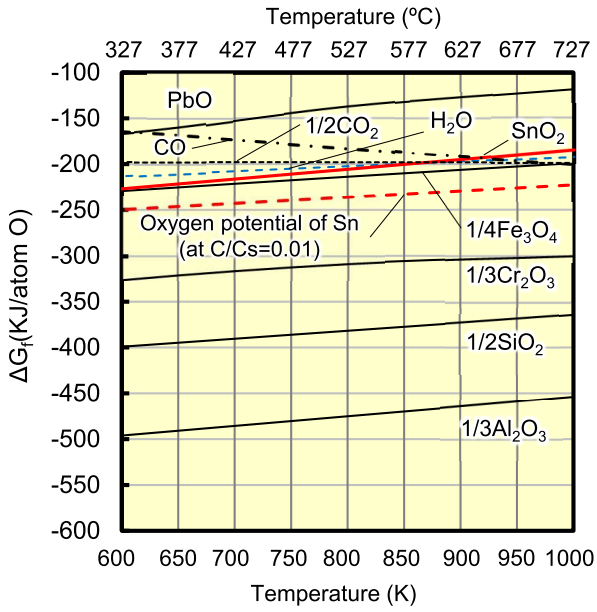

Fig. 7 Relationship between chemical potential of oxygen in liquid Sn and standard Gibbs free energy for formation of some oxides [17].

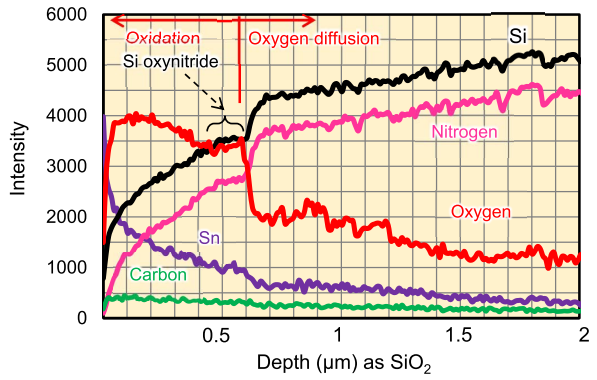

Fig. 8 Result of AES analysis on Si_3N_4 specimen after exposure to liquid Sn at 773 K for 262 hr.

the low oxygen concentration. The standard Gibbs free energy for formation of SnO_2 per oxygen atom is rather large as it is −205.5 kJ/mol at 800 K. The oxidation of SiC in liquid Sn along eq. (1) is reasonable after considerations on these thermodynamic conditions. The thickness of the oxidation layer was approximately 3 μm. The metal elements such as Fe, Cr, and Ni dissolved from the crucible accumulated on the Al_2O_3 specimen surface in liquid Sn [8]. However, such an accumulation was not detected on the surface of SiC specimens.

Figure 8 shows the result of AES analysis of the Si_3N_4 specimen after the corrosion test. Oxygen was detected on the specimen surface, and it diffused into the matrix. The surface could be oxidized in liquid Sn as,

$$Si_3N_4 + 6O_{(Sn)} \rightarrow 3SiO_2 + 4N_{(Sn)}. \quad (3)$$

The standard Gibbs free energies for formation of Si_3N_4

and SiO_2 at 800 K are −485.8 kJ/mol and −763.5 kJ/mol, respectively [17]. The chemical affinity of nitrogen with liquid Sn may be poor, since Sn hardly forms its nitride. Atomic nitrogen is chemically unstable in liquid Sn and its chemical potential must be high. The oxidation of Si_3N_4 in liquid Sn along eq. (3) is reasonable after the considerations on these thermodynamic conditions.

Nitrogen atoms might diffuse into liquid Sn. The depth of oxidized region was approximately 600 nm, and the inward diffusion of oxygen atoms into the matrix was detected in a depth of 2 μm from the surface. Sn diffusion into the oxidized region was detected. The oxidation layer contained nitrogen and Sn, and might exist as silicon oxynitride Si_2N_2O [18] as;

$$Si_3N_4 + Si + 2O_{(Sn)} \rightarrow 2Si_2N_2O. \quad (4)$$

The silicon oxynitride layer might be oxidized according to the continuous supply of oxygen from liquid Sn as;

$$2Si_2N_2O + 3O_2 \rightarrow 4SiO_2 + 4N_{(Sn)}. \quad (5)$$

3.3 Alloying corrosion of Ti in liquid Sn

The Ti specimen could not be removed from the crucible after the corrosion test, though liquid Sn was removed from the crucible as shown in Fig. 5 (d). The specimen was bonded with the crucible due to its alloying corrosion. The specimen and the crucible were cut longitudinally, and the surface cross section of the specimen was metallurgically analyzed.

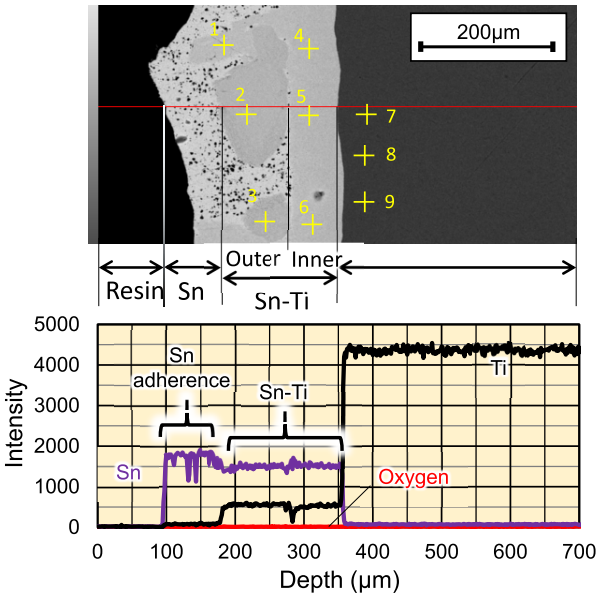

Fig. 9 Cross sectional SEM/EDX analysis of Ti specimen after exposure to liquid Sn at 773 K for 262 hr.

Figure 9 shows the result of SEM/EDX cross sectional analysis at the interface between Sn and Ti. Typical alloying reaction layers [4] were detected as multiple layers on the specimen surface. The inner and outer layers were clearly distinguished in the SEM image. The inner layer had uniform thickness of approximately 75 μm. The outer layer included chunky phases about ~100 um in size. The results of EDX point analysis on the reaction layers were presented in Table 2 and indicated that Sn/Ti in atomic % is approximately 1.6 both for the inner and outer layer. This Sn/Ti ratio is close to the stoichiometric composition of Sn_3Ti_2, in which the Sn/Ti ratio is equal to 1.5. The fragments of Sn_3Ti_2 were formed due to the alloying reaction between Sn and Ti dissolved from the specimen surface, and they were collected in a laminar shape in the outer layer. The inner Sn_3Ti_2 layer formed by Sn diffusion into the Ti matrix. Continuous supply of Sn into the Ti matrix resulted in the formation the Sn_3Ti_2 layer on the specimen surface, which had the highest Sn concentration among the intermetallic compounds of Sn-Ti system.

3.4 Corrosion resistance of Mo and W [16] in liquid Sn

The Mo specimen was totally covered by Sn. The wettability of Mo in liquid Sn was good. The good wettability may achieve a good thermal contact with liquid Sn. The mass loss of the Mo specimen due to the corrosion was 3.14×10^{-3} g (9.1 g/m^2), and corresponded to 0.253% of the initial mass. The corrosion rate was obtained as approximately 31 μm/year, and this rate was much smaller than that of steels. Neither the alloying layer nor oxidation layer was detected on the surface. These corrosion resistant features were almost the same with those of unalloyed W [16].

3.5 Results of liquid Sn contact test

Figure 10 shows the results of liquid Sn dripping test. The temperature of the Al plate locally increased to 560 K from 323 K by the liquid Sn dripping. The surface temperature gradually decreased, and liquid Sn solidified on the Al plate. The solidified Sn did not adhere on the plate sur-

Table 2 Atomic ratio of Sn to Ti in reaction layer formed on Ti specimen in liquid Sn at 773 K for 262 hr (Point number indicates the position shown in SEM image of Fig. 9).

		EDX point analysis								
	Sn_3Ti_2 (Stoichiometric composition)	1	2	3	4	5	6	7	8	9
		Outer layer			Inner layer			Ti matrix		
Sn(at%)/Ti(at%)	1.5	4.54	1.58	1.59	1.86	1.73	1.76	2×10^{-3}		

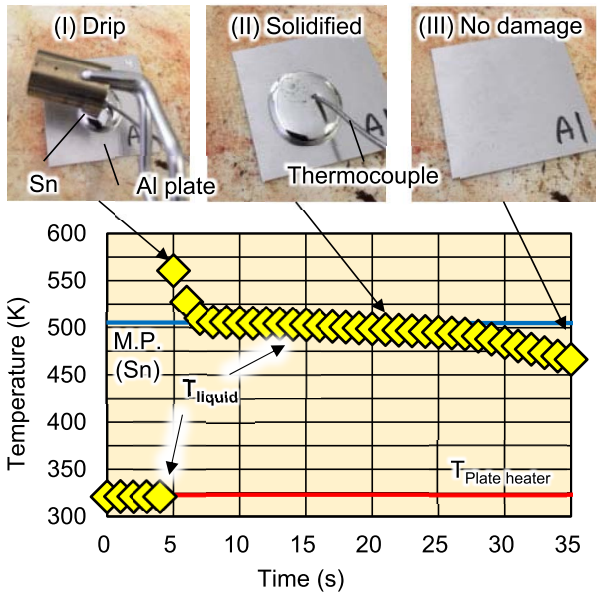

Fig. 10 Result of liquid Sn dripping experiment.

face, and it was easily removed from the plate. No damage of the plate was visually detected in this test.

4. Conclusions

Major conclusions are follows;

1. The conceptual design of the liquid Sn rabbit capsule was developed for the compatibility test of ODS FeCrAlZr alloy under neutron irradiation in HFIR at ORNL.
2. Unalloyed Ti severely corroded in liquid Sn at 773 K due to the formation of intermetallic compound of Sn_3Ti_2.
3. SiC thermometry is used to monitor the temperature in the irradiation test. The corrosion of SiC in liquid Sn at 773 K was negligibly small, though its surface was slightly oxidized.
4. SiC, Si_3N_4, Mo, and W revealed corrosion resistance in liquid Sn at 773 K. They are suitable as the internal holder materials for the test capsule. The wettability of Mo and W in liquid Sn was high. They may have good thermal contact with liquid Sn.
5. The Al plate revealed damage tolerance for liquid Sn contact at 323 K for a short time. Al and its alloy are suitable materials for the capsule housing.

Acknowledgement

This research is supported by Japan and US joint research project “FRONTIER”. This research was partially funded by the U.S. Department of Energ’s Office of Fusion Energy Sciences. Authors would like to acknowledge Dr. Bill Wiffen of ORNL for his support on FRONTIER TASK3 activity and his fruitful discussions on the liquid Sn rabbit capsule design. Authors would acknowledge Mrs. Yoshie Tamai for her technical assistance on corrosion tests in liquid Sn. Authors also would acknowledge Dr. Tada for his technical assistance on metallurgical analysis of specimens tested in liquid Sn.

[1] R.E. Nygren and F.L. Tabares, Nucl. Mater. Energy **9**, 6 (2016).
[2] J. Miyazawa *et al.*, Fusion Eng. Des. **125**, 227 (2017).
[3] M. Kondo and Y. Nakajima, Fusion Eng. Des. **88**, 2556 (2013).
[4] M. Kondo, M. Ishii and T. Muroga, Fusion Eng. Des. **98**, 2003 (2015).
[5] A. Heinzel, A. Weisenburger and G. Müller, Materials and Corrosion **9999**, 1 - 7, maco. 201609211 (2017).
[6] M. Kondo and M. Takahashi, J. Nucl. Mater. **356**, 203 (2006).
[7] B.A. Pint, J. Nucl. Mater. **417**, 1195 (2011).
[8] M. Kondo *et al.*, Fusion Eng. Des. **146**, 2450 (2019).
[9] F.W. Clinard, Jr. and G.F. Hurley, J. Nucl. Mater. **108&109**, 655 (1982).
[10] Y. Hatano *et al.*, J. Plasma Fusion Res. **96**, 3, 145 (2020).
[11] A.A. Campbell, W.D. Porter, Y. Katoh and L.L. Snead, Nucl. Instrum. Methods Phys. Res. B, **370**, 49 (2016).
[12] R.A. FORREST and M.R. GILBERT, “FISPACT-2005: User Manual”, UKAEA FUS 514, United Kingdom Atomic Energy Authority.
[13] L.R. Greenwood *et al.*, DOE/ER-0313/23, Oak Ridge National Laboratory.
[14] M. Takahashi and M. Kondo, Prog. Nucl. Energy **53**, 1061 (2011).
[15] J.R. Lance and G.A. Kenmeny, Am. Soc. Metals. Trans. Quart. **56**, 204 (1963).
[16] N. Kawano, Y. Tamai and M. Kondo, Plasma Fusion Res. **15**, 1205068 (2020).
[17] Thermodynamic database MALT group. Thermodynamic database MALT for Windows. Kagaku Gijutsu-Sha. 2005. (CD-ROM), available from http://www.kagaku.com/malt/index.html (accessed 2020-12-28).
[18] K.L. Luthra, J. Am. Ceram. Soc. **74**, 5, 1095 (1991).